Depolarization of femtosecond pulses in air by nonlinear mechanisms

Daniela A. Georgieva

Daniela A. Georgieva, "Depolarization of femtosecond pulses in air by nonlinear mechanisms ," Proc. SPIE 11047, 20th International Conference and School on Quantum Electronics: Laser Physics and Applications, 110471A (29 January 2019); doi: 10.1117/12.2519307

SPIE.

Event: International Conference and School on Quantum Electronics "Laser Physics and Applications": ICSQE 2018, 2018, Nessebar, Bulgaria

Depolarization of femtosecond pulses in air by nonlinear mechanisms

Daniela A. Georgieva[a,b]

[a]Faculty of Applied Mathematics and Computer Science, Technical University of Sofia, 8 Kliment Ohridski Blvd., 1000 Sofia, Bulgaria
[b]Institute of Electronics, Bulgarian Academy of Sciences, 72 Tzarigradsko shossee, 1784 Sofia, Bulgaria

ABSTRACT

In recent experiments in air with femtosecond pulses significant depolarization effects in nonlinear regime were observed. We use the generalized cubic type nonlinearity and investigate how this operator influences the vector field polarization. A vector set of nonlinear differential equations describing the evolution of the main and signal is derived. The polarization properties of the components of vector fields are investigated numerically.

Keywords: Depolarization, cubic type nonlinearity, ultra-short laser pulses

1. INTRODUCTION

It is well known that during nonlinear propagation in isotropic materials the nano- and picosecond laser pulses preserve their linear and circular polarizations. In the case of elliptical polarization the electrical field vector rotates proportionately to the differences of the intensities and the phases between the E_x and E_y components[1-3]. The rotation of the field vector is homogeneous over while beam spot profile. The preserving of linear and circular polarization and vector rotation in the elliptical case are results of Maker and Therhune (MT) type nonlinear operator, describing propagation of narrow band (*ns* and *ps*) laser pulses.

In recent experiments in air with femtosecond pulses significant depolarization effects were observed[4]. These results cannot be obtained by MT type approximation. For this reason we use the generalized cubic nonlinearity of the type $n_2\left(\vec{E}\cdot\vec{E}\right)\vec{E}$ and investigate how this nonlinearity influences on the vector filed polarization. We found that the generation of optical signal wave spectrally shifted with GHz delay towards the higher frequencies is possible[5]. To investigate the polarization properties in the process of such generation we derive a 3*D*+1 vector system of nonlinear differential equations describing the evolution of the main and signal waves. This system is investigated numerically. The numerical simulations show that the rotation angle of the electrical field vector is different at each point of the spot with maximum in the pulse center.

2. POLARIZATION PROPERTIES OF NARROWBAND PULSES

The propagation of picoseconds laser pulses is described correctly in the frames of Maker and Therhune type polarization

$$P_{nl}^{MT}=n_2\left[\left(\vec{E}\cdot\vec{E}^{*}\right)\vec{E}+\left(\vec{E}\cdot\vec{E}\right)\vec{E}^{*}\right] \tag{1}$$

where n_2 is the nonlinear refractive index. The electrical field $\vec{E}$ at one carrying frequency ω_0 has *x* and *y* components and can be presented by

$$\vec{E}=\frac{A_x\exp\left[i\left(k_0z-\omega_0t\right)\right]+c.c}{2}\vec{x}+\frac{A_y\exp\left[i\left(k_0z-\omega_0t\right)\right]+c.c}{2}\vec{y}, \tag{2}$$

where A_x and A_y are the amplitude components of the pulse. The corresponding nonlinear system of amplitude equations written in dimensionless form and Galilean coordinate system ($z' = z - v_{gr}t$; $t' = t$) is

20th International Conference and School on Quantum Electronics: Laser Physics and Applications, edited by Tanja Dreischuh, Latchezar Avramov, Proc. of SPIE Vol. 11047, 110471A
© 2019 SPIE · CCC code: 0277-786X/19/$18 · doi: 10.1117/12.2519307

$$-2i\frac{\partial A_x}{\partial t}=\Delta_\perp A_x-\beta\frac{\partial^2 A_x}{\partial z^2}+\gamma\left[\left(\left|A_x\right|^2+\frac{2}{3}\left|A_y\right|^2\right)A_x+\frac{1}{3}A_x^*A_y^2\right],$$
$$-2i\frac{\partial A_y}{\partial t}=\Delta_\perp A_y-\beta\frac{\partial^2 A_y}{\partial z^2}+\gamma\left[\left(\left|A_y\right|^2+\frac{2}{3}\left|A_x\right|^2\right)A_y+\frac{1}{3}A_y^*A_x^2\right] \quad (3)$$

where $\gamma=k_0^2d_0^2\tilde{n}_2\left|A_0\right|^2$ is the nonlinear coefficient, $\tilde{n}_2=\frac{3}{8}n_2$, k_0 is the main wave number, d_0 is the waist, $\beta=z_{diff}/z_{disp}=k_0v_{gr}^2k_0''$, $z_{diff}=k_0d_0^2$ is the diffraction length, $z_{disp}=\frac{t_0^2}{k_0''}$ is the dispersion length, v_{gr} is the group velocity, k_0'' is the group velocity dispersion. The last nonlinear terms in equations (3) correspond to the degenerate four-photon parametric mixing (FPPM) processes.

The rotation of the electrical field is connected with the energy exchange between the amplitude components A_x and A_y of the pulse due to FPPM. The nonlinear system (4) admits the Manley-Row conservation law of total energy $U(t)$

$$U(t)=U_x(t)+U_y(t)=\text{const}, \quad (4)$$

where $U_x(t)=\iiint_V\left|A_x\right|^2dxdydz$ and $U_y(t)=\iiint_V\left|A_y\right|^2dxdydz$ are energies of the corresponding components of the electrical field. The variation of the energy of each component is presented by the following integrals

$$\frac{\partial U_x(t)}{\partial t}=\frac{1}{3i}\iiint_V\left(A_x^{*2}A_y^2-A_x^2A_y^{*2}\right)dxdydz,\quad \frac{\partial U_y(t)}{\partial t}=-\frac{1}{3i}\iiint_V\left(A_x^{*2}A_y^2-A_x^2A_y^{*2}\right)dxdydz. \quad (5)$$

If we present the components A_x and A_y of the amplitude function through their modules and phases ϕ_x and ϕ_y correspondingly the energy variations (5) of both components take the form

$$\frac{\partial U_x(t)}{\partial t}=-\frac{2}{3}\iiint_V\left|A_x^2\right|\left|A_y^2\right|\sin\left(2\phi_x-2\phi_y\right)dxdydz,\quad \frac{\partial U_y(t)}{\partial t}=\frac{2}{3}\iiint_V\left|A_x^2\right|\left|A_y^2\right|\sin\left(2\phi_x-2\phi_y\right)dxdydz. \quad (6)$$

The energy of each component is constant when $\Delta\phi=2\phi_x-2\phi_y=0$ (i.e. $\phi_x-\phi_y=0$ – the case of linearly polarized pulse) or $\Delta\phi=\pi$ (i.e $\phi_x-\phi_y=\pi/2$ – the case of circularly polarized pulse) and there is no energy exchange between the functions A_x and A_y. *The absence of energy exchange leads to preservation of the linear and circular polarizations.*

When $\Delta\phi=2\phi_x-2\phi_y\neq0$ (i.e the case of elliptically polarized pulse) the energy of each component is not constant and we observe an exchange of energy between the amplitude components approaching its maximum if $\Delta\phi=2\phi_x-2\phi_y=\pi/2$, i.e. if the phase difference is $\phi_x-\phi_y=\pi/4$. *The energy exchange leads to rotation of the electrical field vector in the case of elliptical polarization.*

2.1 Numerical simulations

In order to investigate the polarization dynamics of the electrical field we treat numerically the nonlinear system of differential equations (1) using an algorithm based on the split-step Fourier method.

We simulate numerically the evolution of 300 *ps* laser pulse typical for atmospheric experiments with initial waist d_0 = 3 *cm* and longitudinal (strob) dimension z_0 = 9 *cm* with power slightly above the critical for self-focusing. The numerical experiments are performed with initial conditions in the form of Gaussian pulses

$$A_x=A_x^0\exp\left(-\frac{x^2+y^2+\left(\frac{z}{3}\right)^2}{2d_0^2}\right)\exp(i\varphi),\quad A_y=A_y^0\exp\left(-\frac{x^2+y^2+\left(\frac{z}{3}\right)^2}{2d_0^2}\right), \quad (7)$$

where φ is the phase difference between the components A_x and A_y. The values of the parameters γ and β are $\gamma = 2,\ \beta \cong 0.0002$.

Linear Polarization (φ = 0)

Figure 1 presents vector diagrams of linearly polarized pulse at distances $z = 0$ and $z = 3z_{diff} / 2$. The vector of the amplitude of the electrical field preserves its linear polarization and does not rotate in (x, y) plane. The same polarization dynamics is observed in the case of circular polarization ($\varphi = \pi/2$).

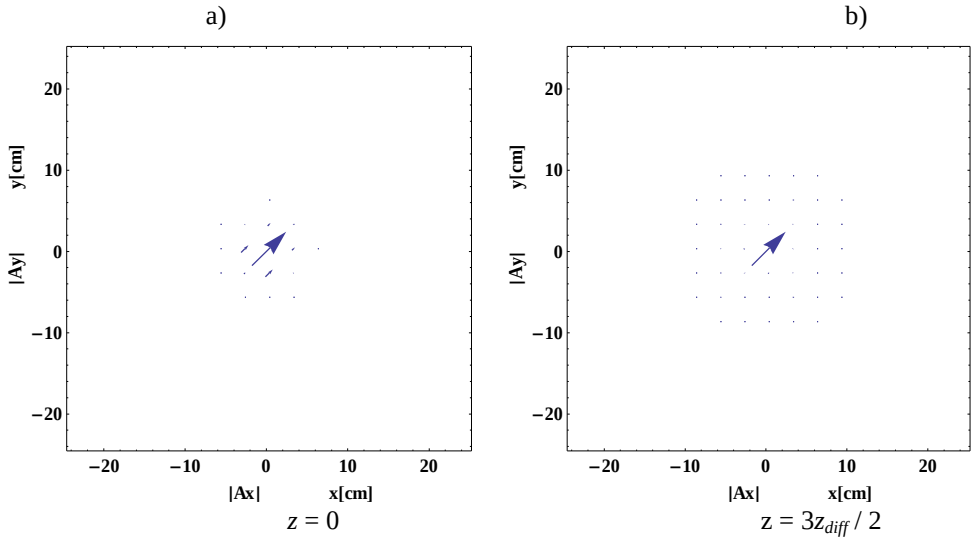

Figure 1. Vector diagrams of the initially linearly polarized laser pulse. Figure 1a) presents the vector diagram of the initial condition. Figure 1b) presents the vector diagram after propagation at a distance $z = 3z_{diff} / 2$. During the nonlinear propagation the vector of electrical field keeps its linear polarization and does not rotate in (x, y) plane.

Elliptical Polarization

Figure 2 presents the time evolution of energy integrals U_x and U_y of elliptically polarized laser pulse with phase difference $\varphi = \pi/4$. We observe an exchange of energy between the amplitude components A_x and A_y due to the degenerate FPPM processes.

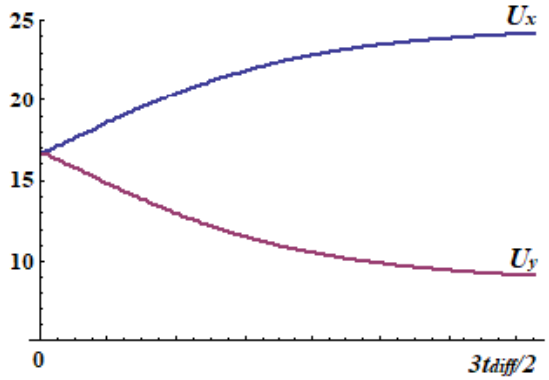

Figure 2. Time evolution of the energy integrals U_x and U_y in the case of elliptically polarized laser pulse. We observe an exchange of energy between the amplitude components A_x (blue) and A_y (red) due to the degenerate four photon parametric mixing processes.

Figure 3 presents vector diagrams of elliptically polarized pulse at distances $z = 0$ and $z = 3z_{diff} / 2$. The vector of the amplitude of the electrical field rotates in (x, y) plane. This rotation is result of the energy exchange between the components A_x and A_y.

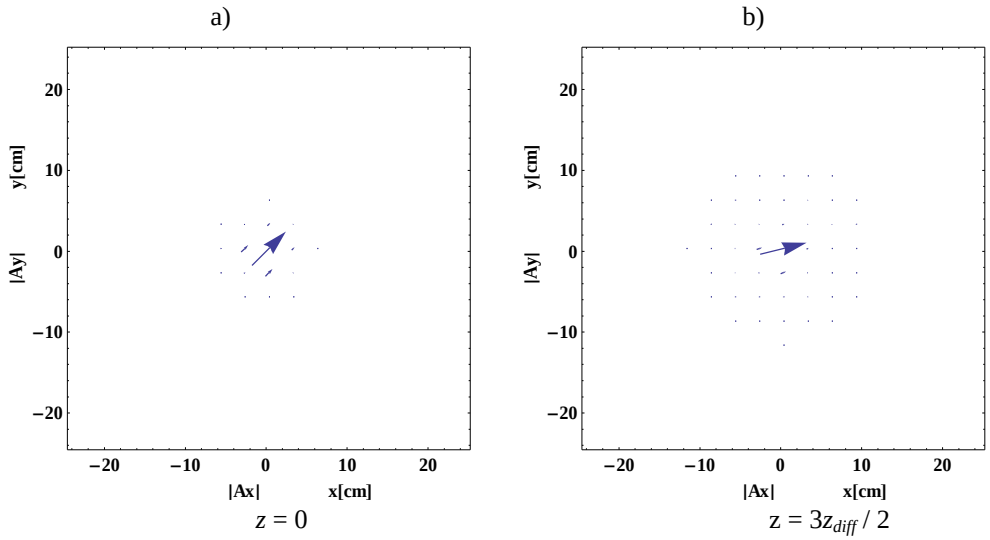

Figure 3. Vector diagrams of the initially elliptically polarized laser pulse. Figure 3a) presents the vector diagram of the initial condition. Figure 3b) presents the vector diagram after propagation at a distance $z = 3z_{diff} / 2$. In this case we observe a rotation of the amplitude vector field in (x, y) plane.

3. POLARIZATION PROPERTIES OF BROADBAND PULSES

In order to investigate the polarization dynamics of broadband laser pulses we use the generalized cubic polarization of the type

$$n_2\left(\vec{E}\cdot\vec{E}\right)\vec{E}\,. \tag{8}$$

The generalized nonlinear operator (8) includes the generation of third harmonic with wave synchronism condition $\omega_s = 3\omega_p$, where ω_p is the main wave (pump) frequency and ω_s is the signal wave frequency. The electrical field $\vec{E}$ has the form $\vec{E} = \vec{E}_p + \vec{E}_s$

$$\vec{E}_p = \frac{A_{px}\exp(i\omega_p t) + A_{px}^*\exp(-i\omega_p t)}{2}\vec{x} + \frac{A_{py}\exp(i\omega_p t) + A_{py}^*\exp(-i\omega_p t)}{2}\vec{y} \tag{10}$$

$$\vec{E}_s = \frac{A_{sx}\exp(i\omega_s t) + A_{sx}^*\exp(-i\omega_s t)}{2}\vec{x} + \frac{A_{sy}\exp(i\omega_s t) + A_{sy}^*\exp(-i\omega_s t)}{2}\vec{y}$$

where $A_{kl}, k = p,s; l = x,y$ are the amplitude functions. More precise analysis shows that the group velocity adds an additional phase (carrier to envelope phase) in the third harmonic terms[4]. Therefore the spectral distance between the pump and the signal wave is with GHz shift in air. Instead on third harmonic $3\omega_p = 3k_0 v_{ph}$ there is a spectral shift to the higher frequencies proportional to the phase-group velocity difference $3\omega_{GHz} = 3k_0\left(v_{ph} - v_{gr}\right)$.

Taking into account the symmetry properties of the nonlinear susceptibility tensor

$$\chi^{(3)}_{xxyy} = \chi^{(3)}_{xyxy} = \chi^{(3)}_{xyyx}, \quad \chi^{(3)}_{ijkl}(3\omega = \omega+\omega+\omega) = 3\chi^{(3)}_{xxyy}, \quad \chi^{(3)}_{ijkl}(\omega = \omega+\omega-\omega) = 2\chi^{(3)}_{xxyy} + \chi^{(3)}_{xyxy} \tag{11}$$

the components of the nonlinear polarization are

$$
\begin{aligned}
P_{nl}^{px} &= \left[|A_{px}|^2 + 2|A_{sx}|^2 + \frac{2}{3}\left(|A_{py}|^2 + |A_{sy}|^2\right)\right] A_{px} + \frac{2}{3}\left[A_{sx}\, A_{sy}^{*} + A_{sx}^{*} A_{sy}\right] A_{py} + \frac{1}{3}\, A_{px}^{*}\, A_{py}^{2} \\
&+ \left[A_{px}^{*2} + \frac{1}{3} A_{py}^{*2}\right] A_{sx} + \frac{2}{3}\, A_{px}^{*}\, A_{py}^{*}\, A_{sy} \\
P_{nl}^{py} &= \left[|A_{py}|^2 + 2|A_{sy}|^2 + \frac{2}{3}\left(|A_{px}|^2 + |A_{sx}|^2\right)\right] A_{py} + \frac{2}{3}\left[A_{sx}\, A_{sy}^{*} + A_{sx}^{*} A_{sy}\right] A_{px} + \frac{1}{3}\, A_{py}^{*}\, A_{px}^{2} \\
&+ \left[A_{py}^{*2} + \frac{1}{3} A_{px}^{*2}\right] A_{sy} + \frac{2}{3}\, A_{px}^{*}\, A_{py}^{*}\, A_{sx} \\
P_{nl}^{sx} &= \left[|A_{sx}|^2 + 2|A_{px}|^2 + \frac{2}{3}\left(|A_{py}|^2 + |A_{sy}|^2\right)\right] A_{sx} + \frac{2}{3}\left[A_{px}\, A_{py}^{*} + A_{px}^{*} A_{py}\right] A_{sy} + \frac{1}{3}\, A_{sx}^{*}\, A_{sy}^{2} \\
&+ \left[A_{px}^{2} + A_{py}^{2}\right] A_{px} \\
P_{nl}^{sy} &= \left[|A_{sy}|^2 + 2|A_{py}|^2 + \frac{2}{3}\left(|A_{px}|^2 + |A_{sx}|^2\right)\right] A_{sy} + \frac{2}{3}\left[A_{px}\, A_{py}^{*} + A_{px}^{*} A_{py}\right] A_{sx} + \frac{1}{3}\, A_{sy}^{*}\, A_{sx}^{2} \\
&+ \left[A_{px}^{2} + A_{py}^{2}\right] A_{py}
\end{aligned}
\tag{12}
$$

The nonlinear terms connected with energy exchange between the pump and signal wave admit wavevector mismatch Δk. We neglect Δk in equations (12) since to a GHZ shift between the waves corresponds $\Delta k \ll 1$.

The system of nonlinear equations resulting from the generalized cubic polarization $n_2\left(\vec{E}\cdot\vec{E}\right)\vec{E}$ in Galilean frame is

$$
-2i\frac{\partial A_{jm}}{\partial t} = \Delta_{\perp} A_{jm} - \beta\frac{\partial^2 A_{jm}}{\partial z^2} + \gamma P_{nl}^{jm}, \qquad j = p, s; \quad m = x, y. \tag{13}
$$

3.1 Numerical simulations

For performing the numerical simulations we use initial 330 *fs* pulse with waist d_0 = 300 μm, longitudinal (strob) dimension z_0 = 100 μm, and spectral width $\Delta\omega^{pulse} >> \Delta\omega^{nl,air} \approx 95$ *GHz*. The numerical experiments are performed with initial conditions in the form of Gaussian pulses

$$
A_{jx} = A_{jx}^{0}\exp\left(-\frac{x^2+y^2+(3z)^2}{2}\right)\exp(i\varphi), \quad A_{jy} = A_{jy}^{0}\exp\left(-\frac{x^2+y^2+(3z)^2}{2}\right), \quad j = p, s. \tag{14}
$$

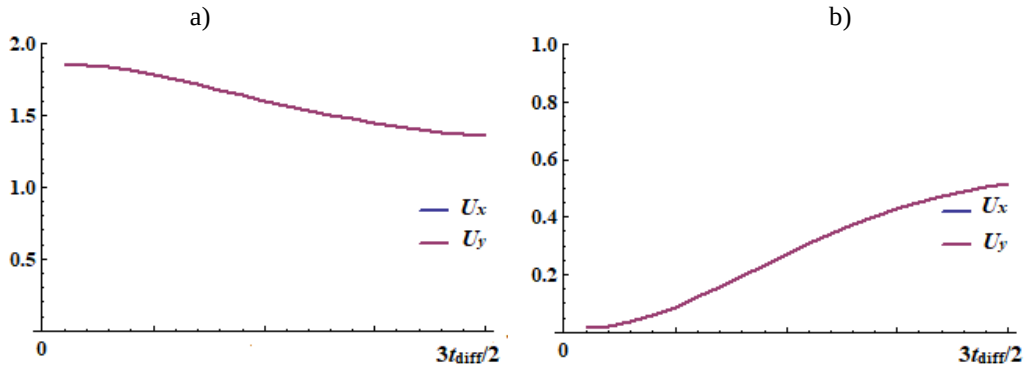

Figure 4. Energy transfer from the pump towards the signal wave is seen from the time evolution of the energy integrals U_x and U_y of main (Fig. 4a) and signal (Fig. 4b) waves in the case of linear polarization. The absence of energy exchange between the components of each wave is the reason for preserving of the linear polarization.

Linear Polarization (φ = 0)

Figure 4 presents the time evolution of energy integrals U_x and U_y of of linearly polarized pulses with initial amplitude parameters $A_{px}^0 = A_{py}^0 = 1$, $A_{sx}^0 = A_{sy}^0 = 0.1$ for $\gamma = 1.1$ and $\beta \cong 0.0002$. In Fig.4a) is plotted the energy of the two components of the pump wave, while in Fig.4b) the energy amplification of signal wave components is shown. An energy transfer from the pump towards the signal wave is observed. An energy exchange between the components of each wave cannot be observed which leads to preserving of the linear polarization (see Fig. 5), i.e. the vector of the amplitude of the electrical field does not rotate in (x, y) plane.

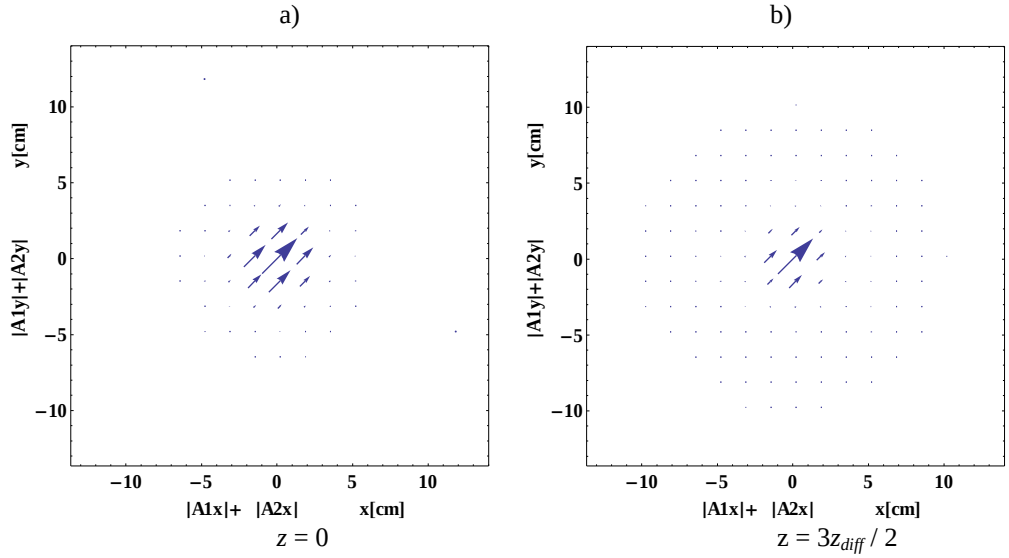

Figure 5. Vector diagrams of the total electrical field in the case of linearly polarized laser pulses. Fig. 5a) presents the vector diagram of the initial condition. Fig. 5b) presents the vector diagram after propagation at a distance of $z = 3z_{diff} / 2$. During the process of amplification of the signal wave the vector of electrical field keeps its linear polarization and does not rotate in (x, y) plane.

Circular Polarization (φ = π/2)

In the ideal case of circular polarization with equal initial pump and signal amplitudes the total electrical field relatively preserves the initial polarization. In the real experiments the main and signal waves have different initial amplitudes. In Fig. 6 the energy integrals U_x and U_y for the following parameters $A_{px}^0 = A_{py}^0 = 1$, $A_{sx}^0 = A_{sy}^0 = 0.3$, $\gamma = 1.8$ and $\beta \cong 0.0002$ are shown.

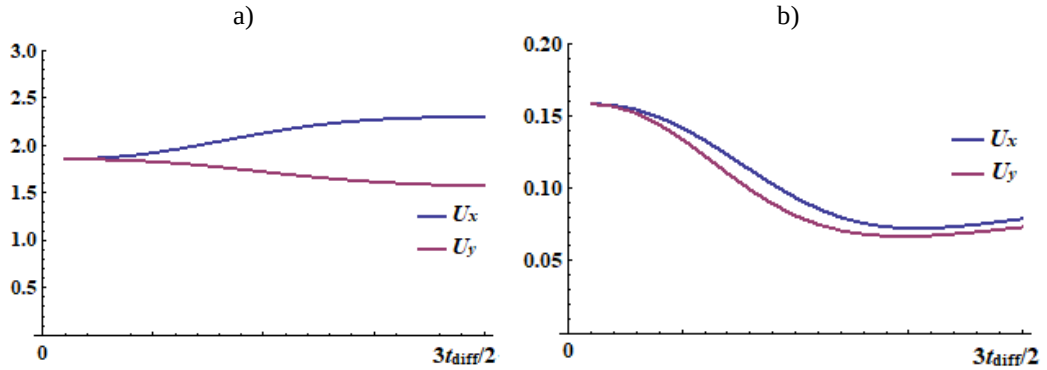

Figure 6. Time evolution of the energy integrals U_x and U_y in the case of circularly polarized laser pulses. We observe an energy transfer between the pump (Fig 6a) and signal pulse (Fig. 6b) with significant exchange of energy between the x and y components of each wave.

An energy transfer between the pump (Fig. 6a) and signal pulse (Fig. 6b) is observed with significant exchange of energy between the *x* and *y* components of each wave. The vector diagrams presented in Fig. 7 show inhomogeneous rotation of the total electrical field vector. The rotation angle is different at each point of the spot with maximum in the pulse center.

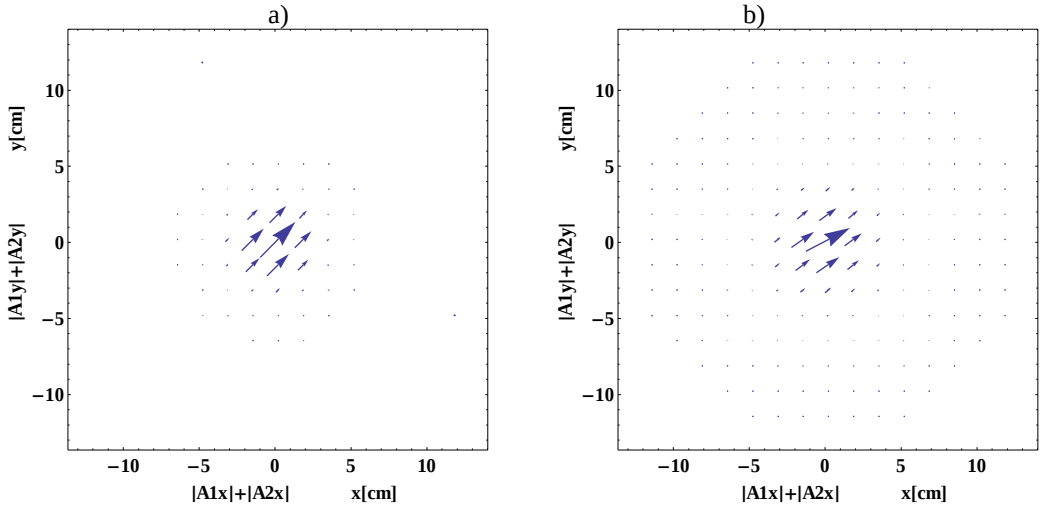

Figure 7. Vector diagrams of the initially circularly polarized laser pulses with different amplitudes. Figure 7a) presents the vector diagram of the initial total vector field. Figure 7b) presents the vector diagram after propagation at a distance $z = 3z_{diff} / 2$. The rotation angle is different at each point of the spot with maximum in the pulse center.

Elliptical Polarization

In our numerical experiments most intense transfer of energy between the main and signal waves as well between their *x* and *y* components (see Fig. 8) is obtained in the case of elliptical polarization. The numerical simulations are performed with phase difference $\varphi = \pi/4$ and initial parameters $A^0_{px} = A^0_{py} = 1$, $A^0_{sx} = A^0_{sy} = 0.1$ for $\gamma = 1.5$ and $\beta \cong 0.0002$.

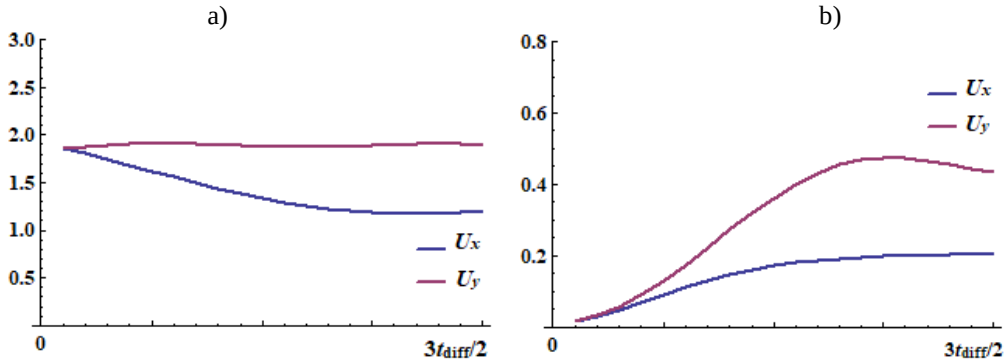

Figure 8. The exchange of energy between the pump and signal wave as well between their *x* and *y* components separately is most intensive in the case of elliptically polarized laser pulses. In Fig. 8a) the evolution of the pump energy integrals U_x and U_y is plotted. Figure 8b) shows the evolution of the signal energy integrals U_x and U_y.

The rotation of the total electrical is most significant in the elliptical case. The vector diagram of the initial electrical field amplitude is plotted in Fig. 9a). Figure 9b) presents the vector diagram after propagation at a distance $z = 3z_{diff} / 2$.

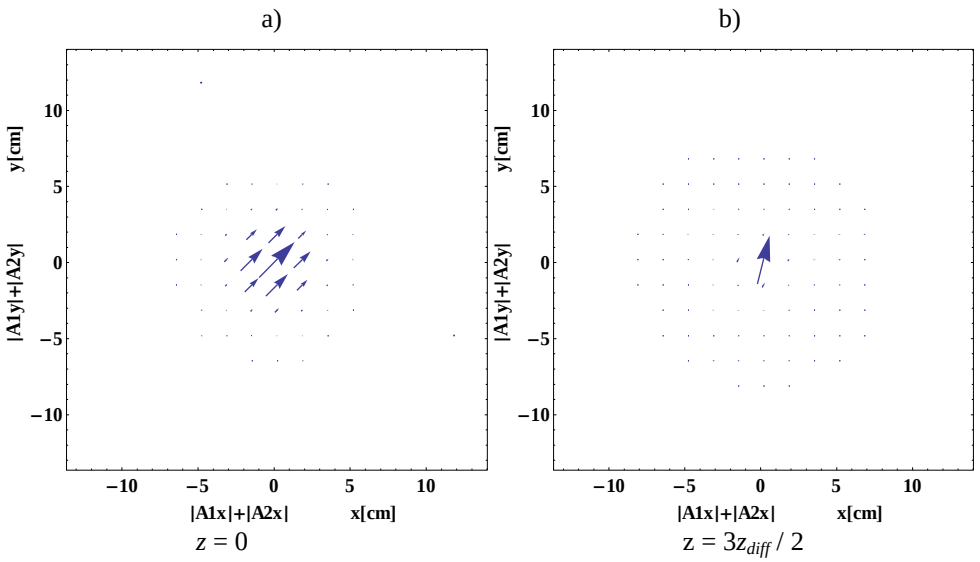

Figure 9. The rotation of the total electrical field is most significant in the elliptical case. The vector diagram of the initial electrical field amplitude is shown in Fig. 9a). Figure 9b) presents the vector diagram after propagation at a distance $z = 3z_{diff} / 2$.

4. CONCLUSIONS

The nonlinear Maker and Therhune type polarization in the nano- and picosecond region preserves the linear and circular polarization of the initial pulse. In the case of elliptical polarization a rotation of the polarization ellipse is observed[2]. The nonlinear generalized cubic type polarization $n_2\left(\vec{E}\cdot\vec{E}\right)\vec{E}$ in the femtosecond region includes the effects of generation of signal wave with GHz spectral shift in air. This leads to depolarization and oscillation of the polarization ellipse of the initially circularly polarized pulse unlike the nano- and picosecond region. The rotation of the total electrical field is most significant in the case of elliptical polarization.

5. ACKNOWLEDGMENTS

The present work is supported from Bulgarian National Science Fund by grant DN 18/11.

REFERENCES

[1] Agrawal, G.P., [Nonlinear Fiber Optics], Academic Press Inc., New York (2007).
[2] Boyd, R.W., [Nonlinear Optics, third edition], Academic Press, New York (2007).
[3] Dakova, A., Kovachev, L., Dakova, D., Georgieva, D., and Slavchev, V.,"Degenerate four-photon parametric processes and vector solitons", Optik 168, 721–727 (2018).
[4] Kosareva, O., et al., "Polarization rotation due to femtosecond filamentation in an atomic gas", Opt. Lett. 35, 2904-2907 (2010).
[5] Georgieva, D., Petrov, T., Yoneda, H., Shikne, R., Nedyalkov, N., and Kovachev, L., "Avalanche parametric conversion and white spectrum generation from infrared femtosecond pulses in glasses", Opt. Express 26, 17649-17661 (2018).